

Printed Microinductors on Flexible Substrates for Power Applications

Erik J. Brandon, Emily E. Wesseling, *Associate Member, IEEE*, Vincent Chang, and William B. Kuhn, *Senior Member, IEEE*

Abstract—A low-profile microinductor was fabricated on a copper-clad polyimide substrate where the current carrying coils were patterned from the existing metallization layer and the magnetic core was printed using a magnetic ceramic-polymer composite material. Highly loaded ferrite-polymer composite materials were formulated, yielding adherent films with $4\pi M_s \approx 3900$ G at $+5000$ Oe applied dc field. These composite magnetic films combine many of the superior properties of high temperature ceramic magnetic materials with the inherent processibility of polymer thick films. Processing temperatures for the printed films were between 100°C and 130°C , facilitating integration with a wide range of substrates and components. The quality factor of the microinductor was found to peak at $Q = 18.5$ near 10 MHz, within the optimal frequency range for power applications. A flat, nearly frequency independent inductance of $1.33\ \mu\text{H}$ was measured throughout this frequency range for a $5\ \text{mm} \times 5\ \text{mm}$ component, with a dc resistance of $2.6\ \Omega$ and a resonant frequency of 124 MHz. The combination of printed ceramic composites with organic/polymer substrates enables new methods for embedding passive components and ultimately the integration of high Q inductors with standard integrated circuits for low profile power electronics.

Index Terms—Inductor, integrated passive components, power electronics, printed electronics.

I. INTRODUCTION

PRINTED electronics are receiving growing attention as a means to integrate microelectronics on a wide variety of substrates. Conventional screen printing [1], [2] as well as ink jet printing [3] have been used to deposit polymer thick film interconnects and resistors [4], [5], organic light emitting diodes [6], solar cells, [7] passive matrix displays [8] and even polymer thin film transistors [9] on both rigid and flexible substrates. These emerging technologies enable the incorporation of electronics onto heat-sensitive substrates for a wide range of potential applications, including electronic paper, electronic labels, flexible smart cards and displays, and inexpensive radio frequency identification (RFID) tags.

Application of printed circuits to fields such as power electronics will require the development of a wider range of materials and processes, to enable the fabrication of higher value

components. This includes low temperature methods to deposit new ceramic based materials, such as high dielectric constant films for capacitors and high permeability soft magnetic films for high Q inductors. Ceramic thin films based on oxides and nitrides are traditionally deposited using a variety of techniques, including sputtering, laser ablation and sol-gel methods. The application of ceramic films is limited in many cases, however, due to the need for high temperature annealing steps. In the case of conventional dielectric and magnetic films, these steps are often critical to develop the microstructure and crystallinity required to achieve adequate materials properties. Furthermore, the brittle nature of these ceramic films along with the mismatch in the coefficient of thermal expansion (CTE) makes integration with flexible substrates impractical.

With the increasing interest in integrated passive components [10], there is a growing need for the development of low-profile or planar magnetic components which can be embedded directly into the substrate and therefore easily integrated with other circuit elements. The miniaturization and integration of magnetic components such as inductors and transformers provides new options in power converter design [11]–[13]. By reducing the physical size of the magnetic components (in conjunction with higher switching frequencies), new distributed, point-of-load power converters can be implemented. Most power related magnetic components, however, require a relatively large volume of material for the core, necessitating thick films which are difficult to achieve using vacuum deposition and other typical thin film processes.

Furthermore, high processing temperatures (which are often in excess of 900°C for conventional ceramic films) severely limit the available substrates which can be used and eliminate the potential for integration with other components. These dual requirements of large volumes of magnetic material and high processing temperatures, which are critical to achieve high Q planar inductors for power applications, have greatly limited the implementation of ceramic magnetic materials in integrated and planar technologies. A new approach to integrated magnetic components is therefore needed to achieve miniaturized inductors with sufficient Q between 1–10 MHz, the critical frequency range for modern switched mode power converters.

II. APPROACH

Two classes of ceramic materials, ferrites and garnets, are commonly used in power and microwave related components for energy storage, isolation and filtering. Specifically, these materials find application in components such as inductors, transformers and circulators. These materials combine the

Manuscript received February 1, 2003; revised June 16, 2003. This work was supported by the Jet Propulsion Laboratory under Contract with the National Aeronautics and Space Administration (NASA). This work was recommended for publication by Associate Editor D. L. Blackburn upon evaluation of the reviewers' comments.

E. J. Brandon, E. E. Wesseling, and V. Chang are with the Jet Propulsion Laboratory, California Institute of Technology, Pasadena, CA 91109 USA (e-mail: erik.brandon@jpl.nasa.gov).

W. B. Kuhn is with the Kansas State University, Manhattan, KS 66506 USA. Digital Object Identifier 10.1109/TCAPT.2003.817641

appropriate magnetic properties with a high resistivity, which are not simultaneously achievable in standard ferromagnetic metals, alloys and glasses.

One approach to the low temperature deposition of thick, ceramic magnetic films is to use screen or stencil printed ceramic-polymer composites, in which ceramic magnetic powders are mixed with a polymer binder. Unlike traditional thick film processes which involve firing the paste at high temperatures to fuse the glass component, these polymer thick films are dried or cured at temperatures less than 200 °C leaving only the magnetic filler and polymer binder. The challenge is to achieve high enough loading fractions of the magnetic ceramic within the diamagnetic polymer binder to achieve a sufficient volume magnetization while still maintaining sufficient adhesion to the substrate. Also, the overall permeability is reduced due to the presence of the diamagnetic polymer through which coupling of the particles must occur, and due to the highly polycrystalline nature of the magnetic material [14]–[25]. The incorporation of distributed gaps between the magnetic particles, however, does have the potential for increasing the saturation field, thereby enhancing the power handling capability of these materials.

The polymer thick film approach developed here offers an alternative to both thin film and traditional thick film hybrid approaches, and combines the often superior properties of high temperature ceramics with the inherent processibility of polymer thick films. Although polymer thick film technologies have been established for conductors, resistors and to a certain extent even capacitors [1], there are limited data available on the properties of polymer thick film magnetic composites, particularly with regard to the use of organic/polymer substrates which can strongly influence component performance [26]–[33]. The ability to combine ceramic films with low temperature substrates opens enormous possibilities for highly integrated power circuits. Combined with the growing use of flexible circuitry, such an approach can find widespread application and can be extended to the development of sensors and devices based on other ceramic materials such as ferroelectrics and piezoelectrics [2].

III. EXPERIMENTAL

The test structures reported herein consisted of a multi-turn planar copper spiral metallization on a flexible polyimide substrate (Fig. 1), with ferrite-polymer composite magnetic thick films printed above and below the plane of the coil (Fig. 2). Fabrication of the microinductors was essentially carried out in a three step process involving

- 1) patterning the copper spiral metallization;
- 2) screen printing the upper magnetic film on top of the copper spiral;
- 3) stencil printing the lower magnetic film on the back of the polyimide, directly below the copper spiral.

The substrate used was 25 μm thick DuPont Pyralux polyimide flexible laminate material with a 17.5 μm layer of copper.

The copper coil, as seen in Fig. 1, consisted of an 11 turn square spiral, with 100 μm wide copper lines and 50 μm spacings, and occupied an area of about 5 mm \times 5 mm (excluding

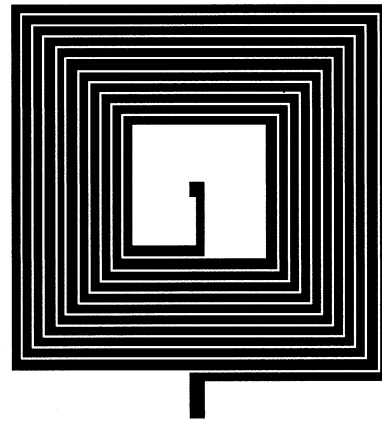


Fig. 1. Layout of the copper inductor, which is comprised of an 11 turn square spiral with 100 μm wide copper lines and 50 μm spacings, occupying an area of about 5 mm \times 5 mm.

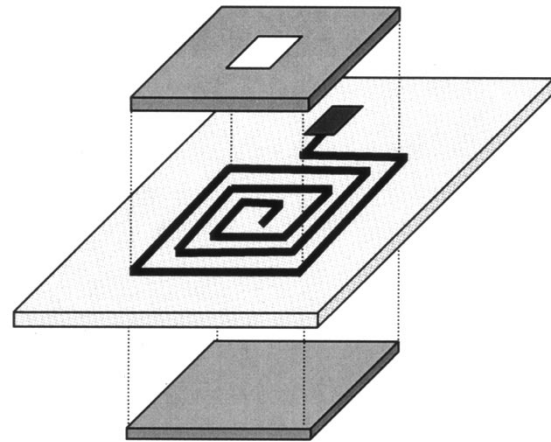


Fig. 2. Exploded view of microinductor structure.

the outer bond pad). The coil was patterned using standard photolithography techniques with an AZ-1518 series photoresist (Shipley). The coil was etched using a ferric chloride solution and the photoresist stripped with acetone. Exposure to the acetone was minimized, to reduce dissolution of the adhesive between the copper and polyimide substrate.

The ink used to print the thick magnetic films was custom formulated (Methode Development Corporation) and was comprised of a thermoplastic resin, solvent, and magnetic filler. A commercially available manganese-zinc ferrite loading powder (Steward 73 300) was used as the magnetic ceramic filler. The average surface area of the powder was 1.4 m^2/g as determined by the BET method, with an average particle size of 10.2 μm as determined by the Coulter method. The saturation moment of the bulk powder was 79.4 emu/g. A highly loaded ink was used to print the ferrite-polymer composite thick films, with the ink containing \approx 4% by mass polymer, \approx 17% by mass solvent and \approx 79% by mass ferrite powder. Rheology of the ink was essentially controlled by adjusting the amount of solvent. Cured films (no solvent) consisted of \approx 96% by mass ferrite, with the balance consisting of polymer. Thermogravimetric analysis was carried out on a TA Instruments Model 2950 Thermogravimetric

Analyzer to determine the optimal curing conditions to achieve the complete evaporation of the solvent.

Screen and stencil printing was carried out on an Automated Production Systems Model SPR-25 Manual Stencil Printer. The upper magnetic film was deposited using off-contact screen printing with an 80 mesh screen with a mesh angle of 30° , a wire diameter of $50\ \mu\text{m}$ and an emulsion thickness of $150\ \mu\text{m}$ (total feature thickness = $200\ \mu\text{m}$). A polymer-based squeegee was used to print the ink through the screen. The upper film was printed through an emulsion opening of about $5\ \text{mm}$ by $5\ \text{mm}$, with a small area in the center left uncovered for access to the bond pad. Typically, excess material was printed around the edges of the bond pad, leaving only the center for access by the probe tips for electrical characterization. Curing consisted of a thermal treatment of the film, to drive off the solvent, and due to the nature of the polymer (a thermoplastic) did not involve any cross-linking. Although a variety of thermal treatments were assessed including oven and hot plate curing, a typical printed film was cured in an oven at $\approx 130^\circ\text{C}$ for 35 min. Higher curing temperatures were found to compromise the adhesion of the film. The ferrite-polymer composite displays negligible conductivity, which serves to electrically isolate the core from the copper coils. The lower magnetic layer was deposited using on-contact stencil printing with a $300\ \mu\text{m}$ thick laser cut stainless steel foil with an opening of about $5\ \text{mm}$ by $5\ \text{mm}$. The ink was printed using a metal squeegee. The film was cured under the same conditions as the upper magnetic film.

Microinductors were initially screened up to 1 MHz on an HP 4284A LCR Meter. Detailed measurements to 200 MHz were made using an HP 8753E vector network analyzer and a GGB Industries model 10 Picoprobe following a standard short-open-load calibration. Step profilometry measurements of printed films were conducted on a Veeco Dektak Surface Profile Measuring System, using thick films printed on a glass slide to achieve optimum planarity. To prepare the sample for profilometry, the slide was dehydrated on a hot plate for five minutes at 100°C to ensure adequate adhesion, and the ink was stencil printed with a metal squeegee using a $300\ \mu\text{m}$ thick foil. In this case, the film was then cured on a hot plate at 100°C for 30 minutes and then oven cured at 100°C for 30 min. A typical stencil printed film had an average thickness of $\approx 300\ \mu\text{m}$ and displayed minimal roughness with an average deviation from the mean line of $<2\%$ (Fig. 3). Multiple profiles were measured on the same film (in directions both parallel and perpendicular to the squeegee print direction), with a typical film displaying a variation in average thickness between measurements of $<1\%$. The surface roughness of the copper used in the Pyralux laminate material is typically within 1–2% of the overall foil thickness (which in this case is $17.5\ \mu\text{m}$) [34]. The surface roughness of the polyimide (in this case Kapton) varies depending on the previous processing history, but for a typical sample is $>30\ \text{nm rms}$ [35]. To ensure a basic level of adhesion, films were typically checked using a qualitative pull test with self-adhesive tape. Isothermal magnetic measurements were made using a Lakeshore Model 7307 vibrating sample magnetometer.

Magnetic measurements were conducted on films printed and processed under a variety of conditions. For the magnetic data

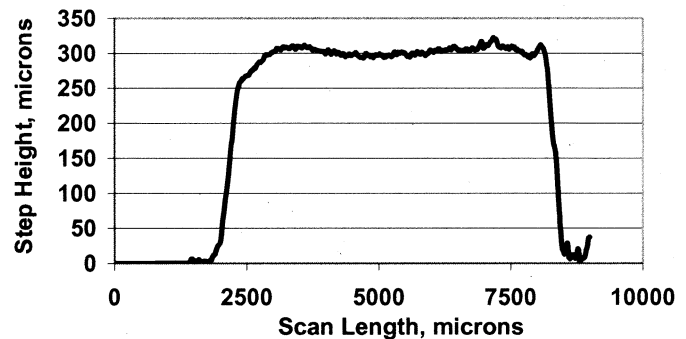


Fig. 3. Profilometer scan of printed composite film. The film was stencil printed on glass using a $300\ \mu\text{m}$ foil with a $5\ \text{mm} \times 5\ \text{mm}$ aperture. Curing schedule was 30 min at 100°C on a hot plate followed by 30 min in an oven at 100°C .

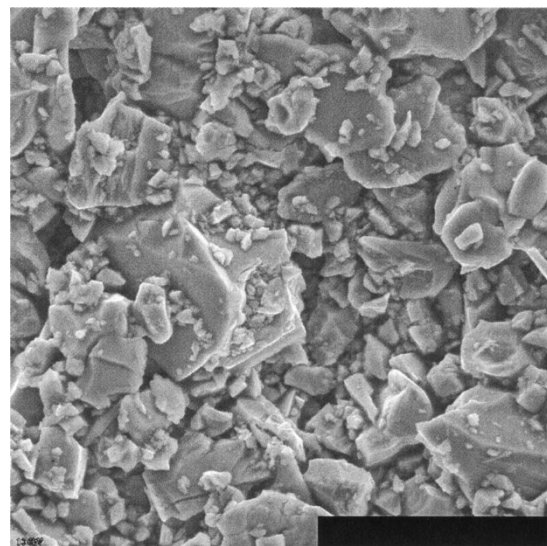


Fig. 4. Scanning electron micrograph of printed composite film normal to the surface, with 10 kV beam and 5000 X magnification. Bar is $10\ \mu\text{m}$.

reported herein, the film was printed on a polyimide substrate with no copper. The substrate was dehydrated on a hot plate for 5 min at 100°C , and the ink was stencil printed with a metal squeegee using the $300\ \mu\text{m}$ foil. The film was then cured on a hot plate at 100°C for 60 min. The film was then cut from the substrate, mounted with vacuum grease to the sample rod facing downward, and manually centered in the applied field. The same film was used for scanning electron microscopy (SEM), which was carried out on a Hitachi S4000 Field Emission Gun SEM using a 10 kV beam.

IV. RESULTS

A step profilometry scan of a stencil printed film on glass is given in Fig. 3, which indicates a film with slightly sloping profiles. A top view scanning electron micrograph of a film printed on polyimide is given in Fig. 4, and shows that although the particles are in intimate contact, there is indication of significant porosity. Vibrating sample magnetometer data taken at room temperature are given in Fig. 5. Due to the surface roughness of the films and the sloped film profiles which make determination of a true film volume difficult, the data is reported as the

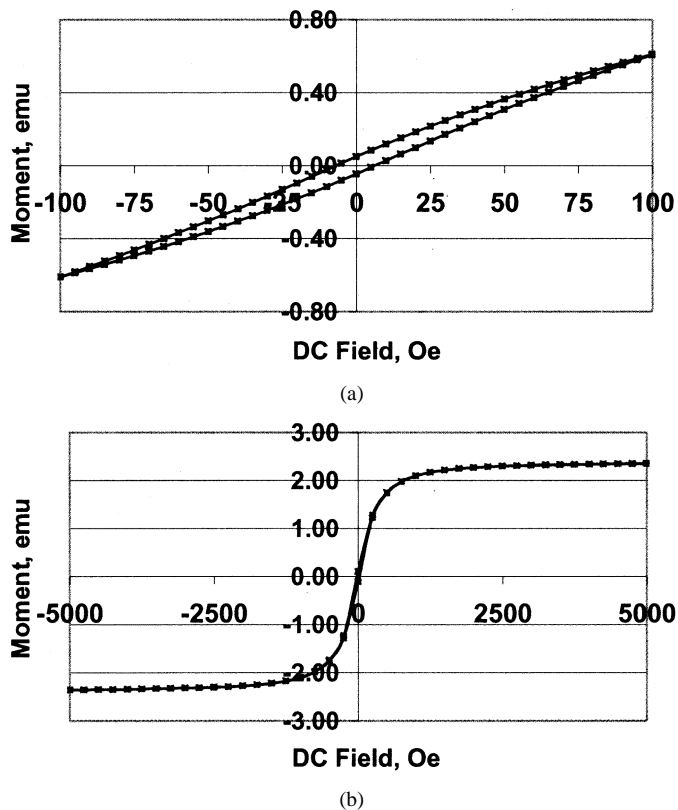


Fig. 5. Vibrating sample magnetometer data of printed composite film on a polyimide substrate, cycled between ± 100 Oe (top) and ± 5000 Oe (bottom).

magnetic moment with units of emu. An approximate volume magnetization at saturation ($4\pi M_s$) can be determined using an estimated film thickness of $300 \mu\text{m}$ (based on the profilometry measurements of stencil printed films on glass) and a film area of about 25 mm^2 (the aperture size of the foil), resulting in a volume magnetization at saturation of 3900 G (given a moment of 2.355 emu at $+5000$ Oe). Data is given at low induction values (loop cycled between ± 100 Oe) and higher induction values (loop cycled between ± 5000 Oe). The coercive field varied between 6.6 Oe when cycled between an applied field of ± 100 Oe and 18.5 Oe when cycled between an applied field of ± 5000 Oe.

Air core inductors (with no magnetic composite) displayed an inductance of $0.51 \mu\text{H}$ at 1 MHz. The measured inductance of a magnetic core test device was $1.33 \mu\text{H}$, indicating the enhancement provided by the core is a factor of about 2.6. The $1.33 \mu\text{H}$ inductor's reflection coefficient S_{11} from 30 kHz to 200 MHz is shown on the Smith chart of Fig. 6. The low-frequency coil resistance is about 2.6Ω and the device stays inductive up to a self-resonant-frequency of about 124 MHz. At a typical application frequency of 10 MHz, the impedance is $4.6 + j85 \Omega$, yielding a quality factor of 18.5.

S_{11} measurements converted to inductance L , resistance R , and quality factor Q are shown in Fig. 7 up to the self-resonant-frequency. These graphs show results for two identically-fabricated inductors designed to check reproducibility. Both inductors show peak Q near 20 in the range of 10 to 20 MHz. Inductance is reasonably constant through 20 MHz and peaks at about $3 \mu\text{H}$ near resonance, while resistance monotonically

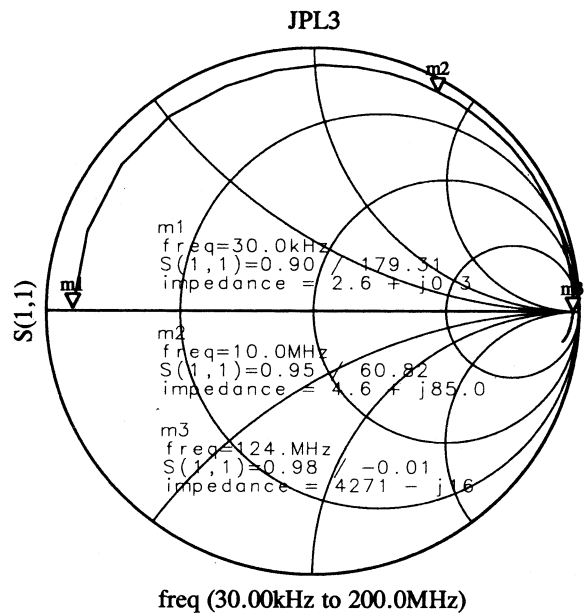


Fig. 6. Measured impedance of $1.33 \mu\text{H}$ inductor with core.

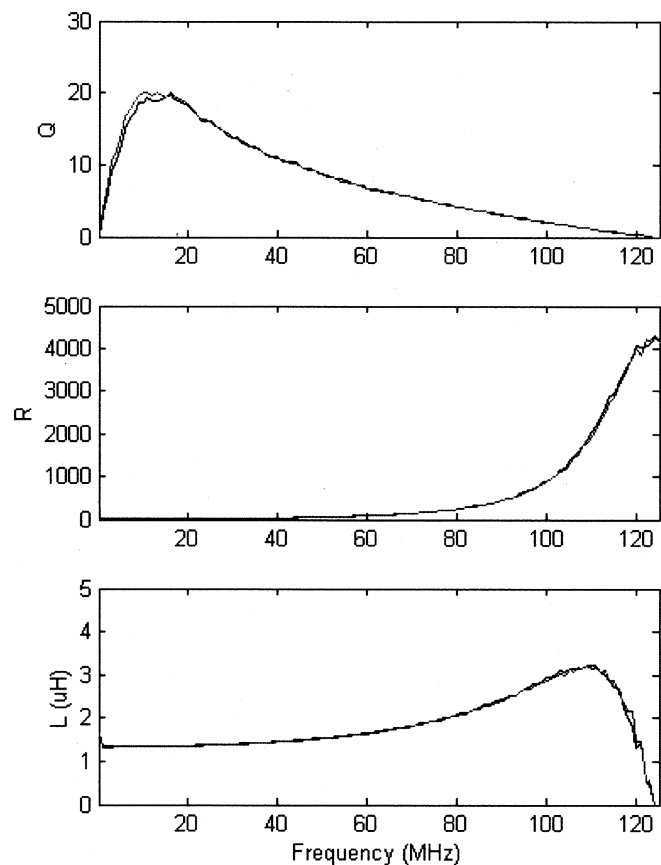


Fig. 7. Inductor performance from 30 kHz to 124 MHz self-resonant-frequency. Two microinductors fabricated under identical conditions are plotted here for comparison.

increases to a peak value of 4270Ω . This variation in series R with frequency and increase in effective L near self-resonance is due to the combined effects of current-crowding [36] and internal (parasitic) capacitance. In particular, Q was defined here simply as reactance divided by resistance, resulting in $Q = 0$ at

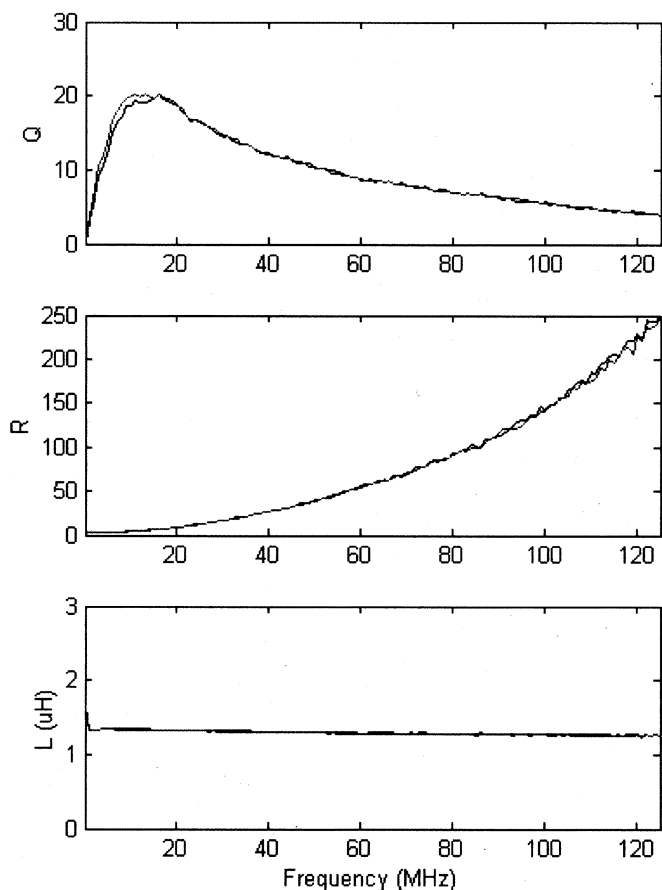


Fig. 8. Corrected performance data after removing effect of parasitic capacitance. Two microinductors fabricated under identical conditions are plotted here for comparison.

self-resonance. For many applications, a definition of Q based on energy storage and dissipation is preferred. This requires the removal of the effects of resonating capacitance from the total impedance.

To estimate the energy-based quality factor, an inductor model consisting of a series R and L , with a parallel C placed across the series combination, was applied. This model was fit to the measured data by converting measured S_{11} to an admittance Y , subtracting off the susceptance of C (found from the low-frequency L value and the self-resonant frequency), and converting the resulting admittance back to impedance. The R and L values found from this impedance are shown in Fig. 8. The inductance is now virtually constant, suggesting a good model-fit. Series resistance increases from its dc value of 2.6Ω up to a maximum of about 250Ω . This increase in R now models ac power losses associated with eddy-currents within the metal traces (current-crowding), and possibly additional losses within the core material. The actual energy-based Q at self-resonance is dependent on these factors and is about 4 in the test inductors.

Finally, an inductor was subjected to a dc bias current during impedance measurements to look for core-saturation effects. The dc bias was provided by an Agilent E3641A supply operating in constant-current mode and was injected into the S-parameter measurement setup through a bias-T. The results are shown in Figs. 9 and 10. Fig. 9 plots dc resistance,

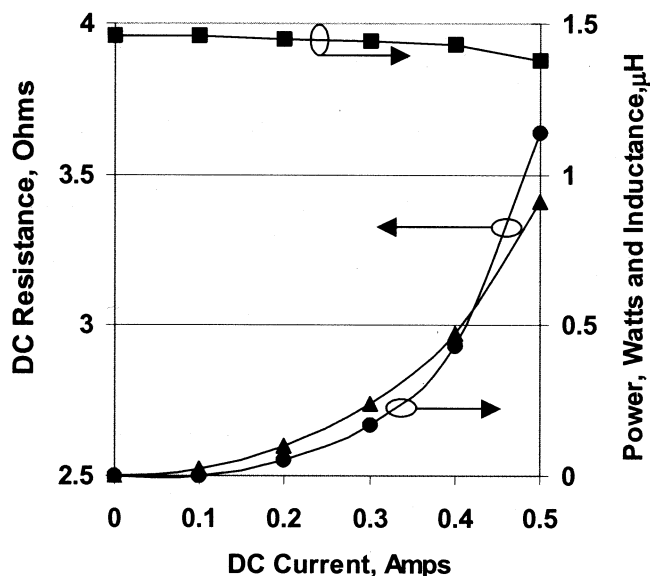


Fig. 9. Effect of bias current on dc series resistance, power dissipation, and inductance.

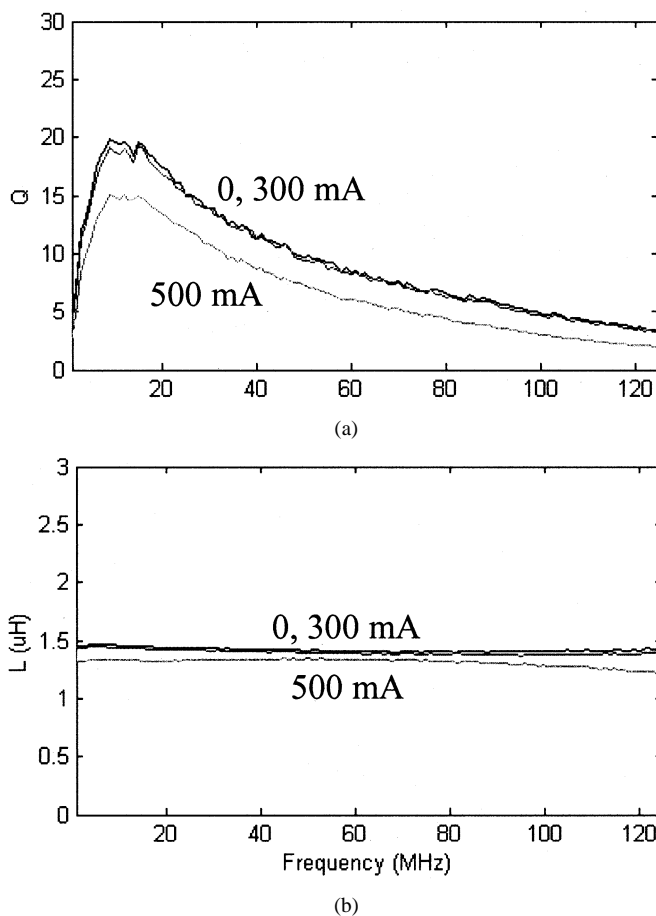


Fig. 10. Inductor performance versus frequency with 0 to 500 mA bias current.

inductance, and power dissipation versus bias current. Power dissipation increases slightly more than quadratically due to increasing dc series resistance as the spiral traces reach higher temperatures. Performance remains good through 300 mA, with little variation in overall inductance, and little decrease in Q (as seen in Fig. 10). At 500 mA, heating of the spiral traces

and core material produces a significant increase in resistance, and a mild reduction in inductance due to the onset of core saturation. The decrease in Q at 500 mA seen in Fig. 10 is in line with values predicted based on a simple increase in series R , further suggesting that core saturation effects are small. Higher currents (e.g., 700 mA) produced thermal-runaway effects where resistance increases did not reach equilibrium, indicating that 500 mA is a practical absolute-maximum specification on operating conditions. Recovery from several cycles of 500 mA testing as well as from temporary overheating caused by thermal runaway was good, with R , L , and Q returning to their original measured values.

V. DISCUSSION

Microinductors fabricated using standard microelectronic fabrication methods and incorporating magnetic films as the core layer have been investigated over the past 20 years [37]–[43]. Most microinductor work previously reported in the literature has focused on using magnetic metallic alloys as the core layers, which are typically sputtered or electroplated and limited in performance due to severe eddy current losses and frequency dependence of the inductance above 1 MHz. More recent work has explored the use of printed pastes on rigid substrates [26]–[33].

The approach reported here features a copper-clad polyimide substrate, a widely available flexible material suitable for microelectronic circuits. By patterning the copper layer on the existing flexible material, a thick metal layer with low resistance was achievable, resulting in a relatively high inductor Q value. Addition of the ferrite-polymer magnetic material to the patterned coil provides a convenient method for rapidly producing planar inductors integrated with a flexible substrate, which suffer minimal loss between 1–10 MHz. Printing the lower magnetic core on the back of the polyimide resulted in sufficient coupling to the upper core and coils to enhance inductance by a factor of 2.6.

Enhancement of the air core inductance with the magnetic core enables the fabrication of a component with $L > 1 \mu\text{H}$, in an area that is smaller than is required for an equivalent air core inductor alone. By keeping the area of the coil relatively small with fewer turns relative to an air core inductor with $L > 1 \mu\text{H}$, a relatively high self-resonant frequency of 124 MHz is achievable (coupled with a suitable Q value near 10 MHz). This is critical, as the operational frequency of the component should be far removed from the resonant frequency. Combined with the use of a magnetic core capable of sustaining an adequate response at 10 MHz, a high Q device can be achieved and operated in the key frequency range for power applications. This is difficult to achieve in a planar configuration, where Q typically peaks in the 1 GHz range for air core inductors with no magnetic core.

One goal in optimizing the process was to minimize the curing time and temperature, as extended temperature soaks degraded adhesion and flexibility. Although the reported microinductors were cured at $\approx 130^\circ\text{C}$ for 35 min in an oven, we found that a curing schedule of 100°C for 60 min on a hot plate was sufficient to drive off 99.5% by mass of the solvent (based on thermogravimetric analysis), yielding adherent films. Using a series of films printed and cured under different temperatures and conditions, no significant influence on magnetic properties

was observed. The only observable influence was on adhesion, which tended to decrease at higher cure temperatures.

The thicknesses of the upper and lower magnetic films differed, due to the difficulty in printing a highly loaded ink through thick screen emulsions that are $>150 \mu\text{m}$. In some cases, the center bond pad was completely covered with ink due to the difficulty in controlling the printing process. Stencil printing of thicker films is easier, and we could readily print $300 \mu\text{m}$ films using a foil. One method to achieve upper and lower magnetic films of equal thickness is to re-distribute the bond pad through the use of an air bridge from the inner pad, enabling both layers to be stencil printed.

We are currently developing methods for quantitatively assessing the mechanical properties of the printed films, particularly with regard to adhesion and flexibility. Qualitatively, the films could sustain minimal flexure, but with a large enough radius of curvature, cracking of the films was observed, accompanied in some cases by complete delamination. Adhesion was adequate, as determined by the self-adhesive tape method, if the cure temperature was kept below 180°C . We are also considering the effects of extended biasing with high currents and self-heating phenomena, as well as aging effects.

VI. CONCLUSION

Ferrite-polymer composite films were successfully combined with copper spiral coil inductors on polyimide substrates to yield a high inductance with good Q in the 1–10 MHz range with a resonant frequency of 124 MHz. Along with polymer thick film resistors and high dielectric capacitors, a wider range of RLC circuits can be fabricated on conventional flexible materials using this approach. Combined with flip chip technology, this approach readily enables integration of active circuitry with embedded passive components on a variety of heat sensitive and flexible substrates.

ACKNOWLEDGMENT

The authors would like to thank F. St. John, Methode Development Corporation, for his valuable assistance in the formulation of the inks, G. Plett, JPL, for the thermal analysis, R. Ruiz, JPL, for the SEM micrograph, E. Kolawa, JPL, for her support of this work, and M. Mojarradi, JPL, for his technical assistance.

REFERENCES

- [1] K. Gilleo, *Polymer Thick Film*. New York: Van Nostrand Reinhold, 1996.
- [2] T. V. Papakostas and N. M. White, "Polymer thick-films on silicon: A route to hybrid microsystems," *IEEE Trans. Comp. Packag. Technol.*, vol. 24, pp. 67–75, Mar. 2001.
- [3] P. Calvert, "Inkjet printing for materials and devices," *Chem. Mater.*, vol. 13, pp. 3299–3305, Oct. 2001.
- [4] A. Dziedzic and A. Kolek, "1/f noise in polymer thick-film resistors," *J. Phys. D. Appl. Phys.*, vol. 31, pp. 2091–2097, Sept. 1998.
- [5] T. V. Papakostas and N. M. White, "Influence of substrate on the gauge factor of polymer thick-film resistors," *J. Phys. D. Appl. Phys.*, vol. 33, pp. L73–L75, July 2000.
- [6] D. A. Pardo, G. E. Jabbour, and N. Peyghambarian, "Application of screen printing in the fabrication of organic light-emitting devices," *Adv. Mater.*, vol. 12, pp. 1249–1252, Sept. 2000.
- [7] S. E. Shaheen, R. Radspinner, N. Peyghambarian, and G. E. Jabbour, "Fabrication of bulk heterojunction plastic solar cells by screen printing," *Appl. Phys. Lett.*, pp. 2996–2998, Oct. 2001.

- [8] J. Birnstock, J. Blassing, A. Hunze, M. Scheffel, M. Stossel, K. Heuser, G. Wittmann, J. Worle, and A. Winnacker, "Screen printed passive matrix displays based on light-emitting polymers," *Appl. Phys. Lett.*, vol. 78, pp. 3905–3907, June 2001.
- [9] H. Siringhaus, T. Kawase, R. H. Friend, T. Shimoda, M. Inbasekaran, W. Wu, and E. P. Woo, "High-resolution inkjet printing of all-polymer transistor circuits," *Science*, vol. 290, pp. 2123–2126, Dec. 2000.
- [10] R. Ulrich and L. Schaper, *Integrated Passive Component Technology*. Piscataway, NJ: IEEE Press, 2003.
- [11] J. G. Kassakian and M. F. Schlecht, "High-frequency high-density converters for distributed power supply systems," *Proc. IEEE*, vol. 76, pp. 362–376, Apr. 1988.
- [12] M. T. Quirke and J. J. Barrett, "Planar magnetic component technology—a review," *IEEE Trans. Comp., Hybrids, Manufact. Technol.*, vol. 15, pp. 884–892, Oct. 1992.
- [13] A. W. Lotfi and M. A. Wilkowski, "Issues and advances in high-frequency magnetics for switching power supplies," *Proc. IEEE*, vol. 89, pp. 833–845, June 2001.
- [14] T. Nakamura, T. Tsutaoka, and K. Hatakeyama, "Frequency dispersion of permeability in ferrite composite materials," *J. Magn. Mater.*, vol. 138, pp. 319–328, Dec. 1994.
- [15] T. Tsutakoka, M. Ueshima, T. Tokunaga, T. Nakamura, and K. Hatakeyama, "Frequency dispersion and temperature variation of complex permeability of Ni-Zn ferrite composite materials," *J. Appl. Phys.*, vol. 78, pp. 3983–3991, Sept. 1995.
- [16] K. C. Han, H. D. Choi, T. J. Moon, W. S. Kim, and K. Y. Kim, "Dispersion characteristics of the complex permeability-permittivity of Ni-Zn ferrite-epoxy composites," *J. Mater. Sci.*, vol. 30, pp. 3567–3570, July 1995.
- [17] B. T. Lee and H. C. Kim, "Prediction of electromagnetic properties of MnZn ferrite-silicon rubber composites in wide frequency range," *Jpn. J. Appl. Phys.*, vol. 35, pp. 3401–3406, June 1996.
- [18] S. S. Kim, S. B. Jo, K. I. Gueon, K. K. Choi, J. M. Kim, and K. S. Churn, "Complex permeability and permittivity and microwave absorption of ferrite-rubber composite in X-band frequencies," *IEEE Trans. Magn.*, vol. 27, pp. 5462–5464, Nov. 1991.
- [19] H. D. Choi, K. S. Moon, I. S. Jeon, W. S. Kim, and T. J. Moon, "Frequency dispersion model of the complex permeability of the epoxy-ferrite composite," *J. Appl. Polym. Sci.*, vol. 66, pp. 477–482, Oct. 1997.
- [20] K. Bober, R. H. Giles, and J. Waldman, "Tailoring of the microwave permittivity and permeability of composite materials," *Int. J. Infrared Millimeter Waves*, vol. 18, pp. 101–123, Jan. 1997.
- [21] M. J. Park and S. S. Kim, "Control of complex permeability and permittivity by air cavity in ferrite-rubber composite and their wide-band absorbing characteristics," *IEEE Trans. Magn.*, vol. 35, pp. 3181–3183, Sept. 1999.
- [22] J. Slama, R. Vican, P. Krivosik, A. Gruskova, and R. Dosoudil, "Magnetic permeability study of composite magnetopolymers," *J. Magn. Mater.*, vol. 196–197, pp. 359–361, May 1999.
- [23] J. H. Paterson, R. Devine, and A. D. R. Phelps, "Complex permeability of soft magnetic ferrite/polyester resin composites at frequencies above 1 MHz," *J. Magn. Mater.*, vol. 196–197, pp. 394–396, May 1999.
- [24] J. Slama, P. Krivosik, R. Dosoudil, R. Vican, A. Gruskova, V. Olah, I. Hudec, and S. Kovacicikova, "The model simulating the magnetic properties of composite polymers," *Int. J. Appl. Electromag. Mech.*, vol. 11, pp. 19–25, 2000.
- [25] F. Mazaleyrat, V. Leger, R. Lebourgeois, and R. Barrue, "Permeability of soft magnetic composites elaborated from flakes of nanocrystalline ribbon," *IEEE Trans. Magn.*, vol. 38, pp. 3132–3134, Sept. 2002.
- [26] R. Kashani, "Formulation, development, and characterization of magnetic pastes and epoxies for thick film inductors," Ph.D. dissertation, Virginia Polytech. Inst. State Univ., Blacksburg, VA, 1992.
- [27] M. M. Riahi-Kashani and A. Elshabini-Riad, "Permeability evaluation of ferrite pastes, epoxies, and substrates over a wide range of frequencies," *IEEE Trans. Instrum. Meas.*, vol. 41, pp. 1036–1040, Dec. 1992.
- [28] J. Y. Park, L. K. Lagorce, and M. G. Allen, "Ferrite-based integrated planar inductors and transformers fabricated at low temperature," *IEEE Trans. Magn.*, vol. 33, pp. 3322–3324, Sept. 1997.
- [29] J. Y. Park and M. G. Allen, "Packaging-compatible microinductors and microtransformers with screen-printed ferrite using low temperature processes," *IEEE Trans. Magn.*, vol. 34, pp. 1366–1368, July 1998.
- [30] S. K. Bhattacharya, J. Y. Park, R. R. Tummala, and M. G. Allen, "Fabrication of a fully integrated passive module for filter application using MCM-D compatible processes," *J. Mater. Sci. Mater. Electron.*, vol. 11, pp. 455–460, Aug. 2000.
- [31] K. I. Arshak, A. Ajina, and D. Egan, "Development of screen-printed polymer thick film planar transformer using Mn-Zn ferrite as core material," *Microelectron. J.*, vol. 32, pp. 113–116, Feb. 2001.
- [32] L. K. Powell, I. Z. Rahman, M. A. Rahman, C. O'Mathuna, and S. O'Reilly, "Development of metallic glass loaded polymer paste," *J. Mater. Processing Technol.*, vol. 119, pp. 318–323, Dec. 2001.
- [33] L. K. Powell, I. Z. Rahman, and M. A. Rahman, "Fabrication of Ni-Zn-Cu ferrite powders and polymer pastes," *Mater. Sci. Forum.*, vol. 373–376, pp. 769–772, 2001.
- [34] *Vendor data (DuPont)*, 2003.
- [35] D. B. Thomasson, M. Bonse, J. R. Huang, C. R. Wronski, and T. N. Jackson, "Tri-layer a-Si:H integrated circuits on polymeric substrates," in *Proc. Int. Electron Devices Meeting Tech. Dig.*, Dec. 1998, pp. 253–256.
- [36] W. B. Kuhn and N. M. Ibrahim, "Analytical modeling of current crowding effects in multi-turn spiral inductors," *IEEE Trans. Microwave Theory Tech.*, vol. 49, pp. 31–38, Jan. 2001.
- [37] R. F. Soho, "Magnetic thin film inductors for integrated circuit applications," *IEEE Trans. Magn.*, vol. MAG-15, pp. 1803–1805, Nov. 1979.
- [38] T. Sato, H. Tomita, A. Sawabe, T. Inoue, T. Mizoguchi, and M. Sahashi, "A magnetic thin film inductor and its application to a MHz switching dc-dc converter," *IEEE Trans. Magn.*, vol. 30, pp. 217–223, Mar. 1994.
- [39] C. R. Sullivan and S. R. Sanders, "Design of microfabricated transformers and inductors for high-frequency power conversion," *IEEE Trans. Power Electron.*, vol. 11, pp. 228–238, Mar. 1996.
- [40] V. Korenivski and R. B. van Dover, "Magnetic film inductors for radio frequency applications," *J. Appl. Phys.*, vol. 82, pp. 5247–5254, Nov. 1997.
- [41] C. H. Ahn and M. G. Allen, "Micromachined planar inductor on silicon wafers for MEMS applications," *IEEE Trans. Ind. Electron.*, vol. 45, pp. 866–876, Dec. 1998.
- [42] J. W. Park, J. Y. Park, Y. H. Joung, and M. G. Allen, "Fabrication of high current and low profile micromachined inductor with laminated Ni/Fe core," *IEEE Trans. Comp. Packag. Technol.*, vol. 25, pp. 106–111, Mar. 2002.
- [43] W. Ruythooren, E. Beyne, J.-P. Celis, and J. De Boeck, "Integrated high-frequency inductors using amorphous electrodeposited Co-P core," *IEEE Trans. Magn.*, vol. 38, pp. 3498–3500, Sept. 2002.

Erik J. Brandon received the B.S. degree in chemistry from Texas Lutheran College, Seguin, in 1991 and the Ph.D. degree in inorganic chemistry from the University of Utah, Salt Lake City, in 1997. His doctoral work focused on the synthesis and characterization of novel molecule-based magnetic materials.

He is a Senior Member of Staff, Materials and Device Technologies Group, NASA Jet Propulsion Laboratory (JPL), Pasadena, CA. He was a California Institute of Technology Post-doctoral Scholar at JPL. He has managed several technology development tasks at JPL, including efforts in microinductors, integrated passive components, microbatteries, and flexible electronics.

Emily E. Wesseling (A'98) received the B.Sc. degree from Ohio State University, Columbus, in 1988 and the Ph.D. degree in physics from the University of Minnesota, Minneapolis, in 1996.

She worked at the Jet Propulsion Laboratory, Pasadena, CA, for six years where her research first focused on vertical Bloch line data storage and later on embedded passive devices.

Vincent Chang is currently pursuing the B.S. degree in electrical engineering at the California Institute of Technology, Pasadena, CA.

William B. Kuhn (S'78–M'79–SM'98) was born in Newport News, VA, in 1956. He received the B.S. degree from the Virginia Polytechnic Institute and State University, Blacksburg, in 1979, the M.S. degree from the Georgia Institute of Technology (Georgia Tech), Atlanta, in 1982, and the Ph.D. degree from the Virginia Polytechnic Institute and State University, Blacksburg, in 1996, respectively, all in electrical engineering.

From 1979 to 1981, he was with Ford Aerospace and Communications Corporation, Palo Alto, CA, where he designed radio receiver equipment including frequency synthesizers and bit synchronizers. From 1983 to 1992, he was with the Georgia Tech Research Institute, working primarily in radar signal analysis and mixed-signal circuit simulator development. In 1996, he joined Kansas State University, Manhattan, as an Assistant Professor, later becoming an Associate Professor in 2000. He currently teaches courses in communications theory, radio and microwave circuit/system design, and VLSI. His research is primarily targeted at low-power radio electronics in CMOS, BiCMOS, and SOI technologies.